ISSN 1392-2114 ULTRAGARSAS, Nr.1(54). 2005.

Shadow moire analysis of surface oscillations of the fluid

M. Ragulskis[1], R. Šatkauskas[2], K. Ragulskis[1], R. Maskeliūnas[3]

[1]*Kaunas University of Technology,*

[2]*Ministry of Environment,*

[3]*Vilnius Gediminas Technical University*

Introduction

The problem of fluid oscillations is common in different engineering applications. Shadow moire is one of the popular methods for experimental analysis of vibrations of the surface of the fluid [1, 2].

There exists a definite need for hybrid numerical – experimental techniques [3, 4] that could help to interpret the measurement results. Such techniques usually comprise a numerical model of the system coupled with optical and geometrical parameters of the measurement set-up. Then the predicted response of an experimental optical measurement system can be mimicked in a virtual numerical environment when the dynamical parameters of the analysed object are pre-defined.

Visualisation techniques of the results from finite element analysis procedures are important due to several reasons. First is the meaningful and accurate representation of processes taking place in the analysed structures. Second, and perhaps even more important, is building the ground for hybrid numerical - experimental techniques. A typical example of FEM application in developing a hybrid technique is presented in [3].

Shadow moiré analysis

The principle of the shadow moire analysis [1, 2] is shown in Fig. 1. *x*, *y* and *z* are the orthogonal Cartesian axes of coordinates (*y* axis is not shown in the figure for the sake of simplicity). The surface of the fluid in the status of equilibrium is in the plane $z = -d$, here *d* is the distance between the moire grating and the surface of the fluid in the status of equilibrium. Moire grating is in the plane $z = 0$ and the photographic plate is parallel to this plane. The deflection of the surface of the fluid is *w*. α is the angle between the *z* axis and the direction of the parallel incident rays of light, *u* is the shift of the shadow moiré grating in the direction of the *x* axis with respect to the initial moiré grating. *H* is the thickness of the layer of the fluid in the status of equilibrium.

The dynamic response of the surface of the fluid is directly related to its eigenmodes. Therefore analysis of natural vibrations taking place according to the eigenmode of the surface of the fluid is important in a number of engineering applications.

The developed technique for construction of shadow moiré images of the eigenvibrations of the surface of the fluid is applicable in a hybrid numerical - experimental shadow moire analysis using the stroboscopic method.

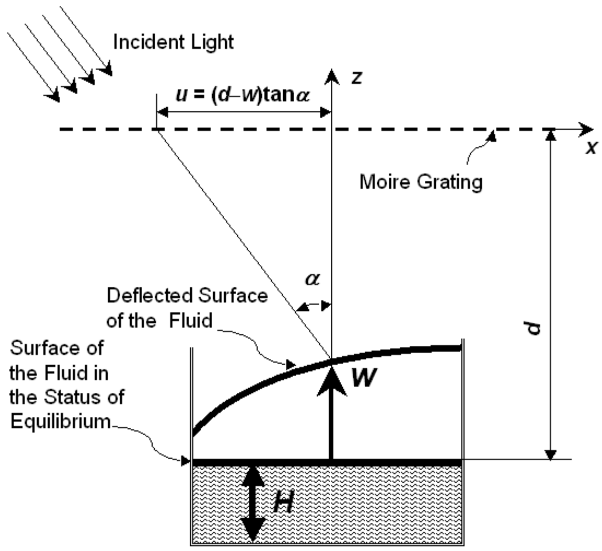

Fig.1. **The schematic of vibration analysis of the surface of the fluid by shadow moiré**.

The vibrations of the fluid are described by the following equation [5, 6, 7]:

$$\frac{\partial^2 w}{\partial t^2} - \frac{\partial}{\partial x}\left(Hg\frac{\partial w}{\partial x}\right) - \frac{\partial}{\partial y}\left(Hg\frac{\partial w}{\partial y}\right) = 0\,, \qquad (1)$$

where *g* is the acceleration of gravity of the earth.

First of all the eigenmodes of the surface of the fluid are calculated. The finite element has one nodal degree of freedom (the displacement *w*). It is assumed that the surface of the fluid performs vibrations according to the eigenmode (the frequency of excitation is about equal to the eigenfrequency of the corresponding eigenmode and the eigenmodes are not multiple). The vibrations of the surface of the fluid are registered stroboscopically when the fluid is in the state of extreme deflections according to the eigenmode.

Then the moiré images are produced [1, 2] assuming that the shadow displacement in the direction of the *x* axis *u* takes the following value:

$$u = (d - w)\tan\alpha\,. \qquad (2)$$

For the more general case it is assumed that the grating makes an angle β with the *x* axis. The parallel rays of light turn together with the grating. Then the intensity of the moiré image takes the form:

$$I = \frac{1}{2}\left(\begin{array}{l} \cos^2\left(\frac{2\pi}{\lambda}(x\cos\beta + y\sin\beta)\right) + \\ + \cos^2\left(\frac{2\pi}{\lambda}\left(\begin{array}{l} x\cos\beta + y\sin\beta - \\ -(d-w)\tan\alpha \end{array}\right)\right) \end{array} \right), \quad (3)$$

where λ is the constant describing the distance between the lines of the grating.

The stiffness matrix of the element describing the vibrations of the surface of the fluid has the form:

$$[K] = \iint [B]^T Hg[B]dxdy \,, \quad (4)$$

where

$$[B] = \begin{bmatrix} \frac{\partial N_1}{\partial x} & \ldots \\ \frac{\partial N_1}{\partial y} & \ldots \end{bmatrix}, \quad (5)$$

and N_i is the i-th shape function of the finite element.

The mass matrix has the following form:

$$[M] = \iint [N]^T [N]dxdy \,, \quad (6)$$

where:

$$[N] = [N_1 \quad \ldots]. \quad (7)$$

Eq. 1 is based on the equations of motion in the directions of the x and y axes:

$$\begin{array}{l} \rho\frac{\partial u^f}{\partial t} + \frac{\partial p}{\partial x} = 0, \\ \rho\frac{\partial v^f}{\partial t} + \frac{\partial p}{\partial y} = 0, \end{array} \quad (8)$$

where ρ is the density of the fluid, u^f and v^f are the velocities of the fluid in the directions of the x and y axes, p is the pressure. It is also based on the equation of static equilibrium in the direction of the z axis:

$$p = \rho g w, \quad (9)$$

and on the equation of continuity for the incompressible fluid with the free surface:

$$\frac{\partial w}{\partial t} + \frac{\partial}{\partial x}\left(Hu^f\right) + \frac{\partial}{\partial y}\left(Hv^f\right) = 0. \quad (10)$$

On the basis of Eq. 8 and 9:

$$-\frac{1}{g}\begin{Bmatrix} \frac{\partial u^f}{\partial t} \\ \frac{\partial v^f}{\partial t} \end{Bmatrix} = \begin{Bmatrix} \frac{\partial w}{\partial x} \\ \frac{\partial w}{\partial y} \end{Bmatrix}, \quad (11)$$

thus the accelerations in the directions of the x and y axes are proportional to the derivatives of w with respect to x and y. For a harmonic motion according to the eigenmode the displacements are proportional to the accelerations. So $\frac{\partial w}{\partial x}$ and $\frac{\partial w}{\partial y}$ fully describe the plane motion of the fluid.

In order to obtain the nodal values of $\frac{\partial w}{\partial x}$ and $\frac{\partial w}{\partial y}$ the procedure of conjugate approximation [8] is used. The values of $\frac{\partial w}{\partial x}$ and $\frac{\partial w}{\partial y}$ at the points of numerical integration of the finite elements are obtained as:

$$\begin{Bmatrix} \frac{\partial w}{\partial x} \\ \frac{\partial w}{\partial y} \end{Bmatrix} = [B]\{\delta\}, \quad (12)$$

where $\{\delta\}$ stands for the vector of nodal values of w for the analysed finite element. Then the nodal values of $\frac{\partial w}{\partial x}$ and $\frac{\partial w}{\partial y}$ are obtained by solving the following systems of linear algebraic equations:

$$\begin{array}{l} \left[\Sigma\left(\iint [N]^T [N]dxdy\right)\right] \cdot \left[\{\delta_x\} \quad \{\delta_y\}\right] = \\ = \Sigma\left(\iint [N]^T \left[\frac{\partial w}{\partial x} \quad \frac{\partial w}{\partial y}\right]dxdy\right), \end{array} \quad (13)$$

where the summation sign stands for the direct stiffness procedure, the vector columns $\{\delta_x\}$ and $\{\delta_y\}$ are the nodal values of $\frac{\partial w}{\partial x}$ and $\frac{\partial w}{\partial y}$ respectively of the global system.

The relationships presented above form the basis for generation of the shadow moiré images of the surface of the fluid and the analysis described below.

Results of analysis by shadow moiré

A circular channel of constant thickness is analysed. Such configurations of fluid channels are common in lithographic printing devices. The perspective projection of the finite element mesh for the tenth eigenmode is shown in Fig. 2. The mesh in the status of equilibrium is grey and deflected in the direction of the z axis according to the eigenmode is black.

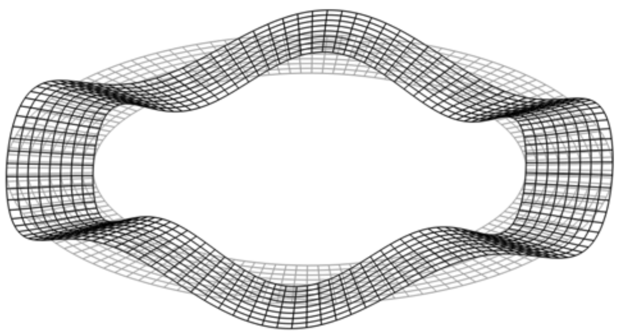

Fig.2. **The perspective projection of the tenth eigenmode of the surface of the fluid (the mesh in the status of equilibrium is grey and deflected in the direction of the *z* axis according to the eigenmode is black).**

Isolines of the displacement of the surface of the fluid in the direction of the z axis for the tenth eigenmode are shown in Fig. 3.

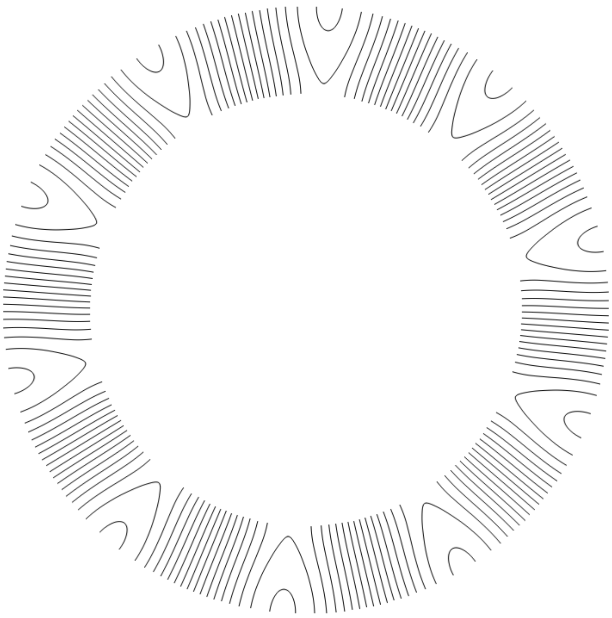

Fig.3. **Isolines of the displacement of the surface of the fluid in the direction of the *z* axis for the tenth eigenmode**.

The stroboscopic shadow moire image of the surface of the fluid in the status of equilibrium is shown in Fig. 4. No fringes are observed in this case and such an image can be used for the initial calibration of the experimental set-up.

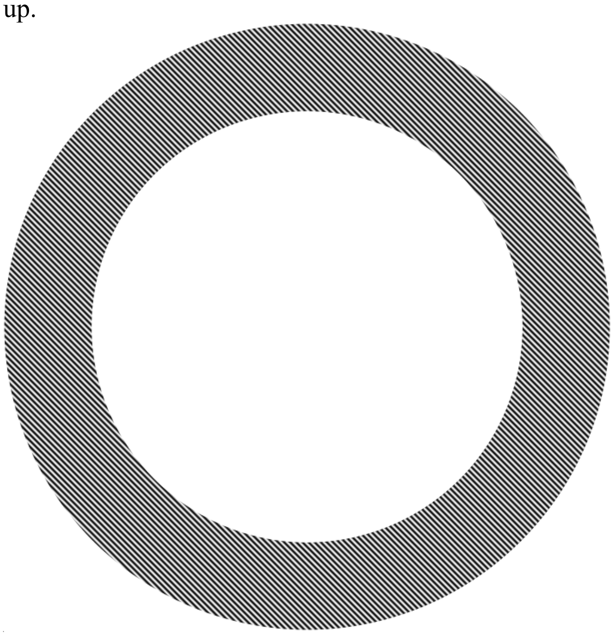

Fig.4. **The stroboscopic shadow moire image of the surface of the fluid in the status of equilibrium**.

The stroboscopic shadow moire image of the tenth eigenmode is shown in Fig. 5. The correspondence of the character of shadow moiré fringes with the drawing of the isolines described previously is evident.

On the basis of the calculated eigenmodes the nodal values of $\frac{\partial w}{\partial x}$ and $\frac{\partial w}{\partial y}$ are obtained by using the conjugate approximation. As mentioned previously the quantities

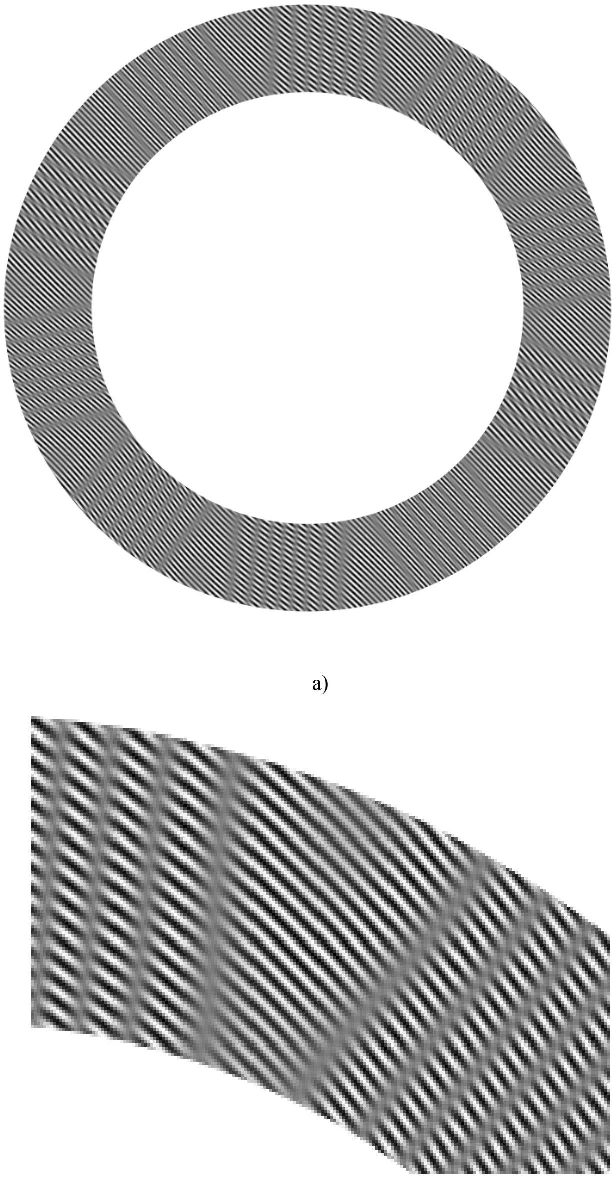

a)

b)

Fig.5. **The stroboscopic shadow moire image of the tenth eigenmode of the surface of the fluid: a – general view; b – zoomed area of the region of maximum deflections**.

$\frac{\partial w}{\partial x}$ and $\frac{\partial w}{\partial y}$ describe the plane motion of the fluid. The finite element mesh for the plane motion for the tenth eigenmode is shown in Fig. 6. The mesh in the status of equilibrium is grey and deflected according to the plane motion is black.

One is to have in mind that the latter result is obtained only from the numerical calculations: thus the concept of hybrid experimental – numerical analysis becomes especially important. In the first stage of the analysis the correspondence of the transverse motions of the fluid obtained from the experimental shadow moiré analysis and by the numerical calculations is determined. If the correlation of those results is acceptable then the plane motion of the fluid is obtained on the basis of numerical calculations as the second stage of the analysis.

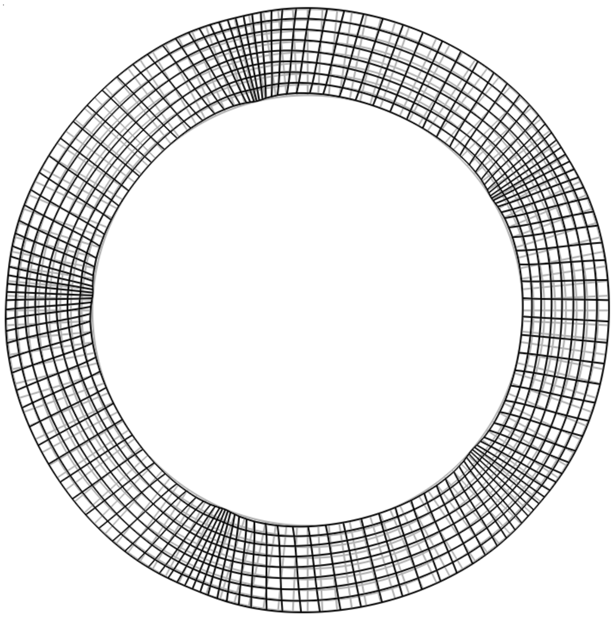

Fig.6. **The finite element mesh for the plane motion for the tenth eigenmode (the mesh in the status of equilibrium is grey and deflected according to the plane motion is black).**

Conclusions

The construction of shadow moire images builds the ground for hybrid numerical-experimental procedures for effective solution of problems of the analysis of vibrations of the surface of the fluid. The stroboscopic shadow moiré images of the eigenmodes of the surface of the fluid are obtained.

The plane motion of the fluid is obtained only from the numerical calculations: thus the concept of hybrid experimental – numerical analysis consists of two stages. In the first stage the correspondence of the transverse motions of the fluid obtained from the experimental shadow moiré analysis and by the numerical calculations is determined. If the correlation of those results is acceptable then the plane motion of the fluid is obtained on the basis of numerical calculations as the second stage of the analysis.

References

1. **Kobayashi A. S.** Handbook on experimental mechanics – 2nd ed.. SEM. 1993.
2. **Post D., Han B., Ifju P.** High sensitivity moiré: Experimental analysis for mechanics and materials. Berlin: Springer Verlag. 1997.
3. **Holstein A., Salbut L., Kujawinska M., Juptner W.** Hybrid experimental-numerical concept of residual stress analysis in laser weldments. Experimental mechanics. 2001. 41(4). P. 343-350.
4. **Soifer V. A.** Computer processing of images. Herald of the Russian Academy of Sciences. 2001. Vol. 71(2). P. 119-129.
5. **Iershov N. F., Shahvierdi G. G.** The method of finite elements in the problems of hydrodynamics and hydroelasticity. Leningrad: Sudostroienie. 1984. P. 240.
6. **Connor J. J., Brebbia C. A.** Finite element techniques for fluid flow. Leningrad: Sudostroienie. 1979. P. 264.
7. **Rao S. S.** The finite element method in engineering. Pergamon Press, U.K. 1982. P. 625.
8. **Segerlind L. J.** Applied finite element analysis. Moscow: Mir. 1979. P. 392.

M. Ragulskis, R. Šatkauskas, K. Ragulskis, R. Maskeliūnas

Skysčio paviršiaus svyravimų analizė šešėlinio muaro metodu

Reziumė

Skysčio paviršiaus svyravimams pagal savąją formą tirti taikomas stroboskopinis šešėlinio muaro metodas. Kaip baigtinių elementų skaičiavimų rezultatas gauti vaizdai naudojami eksperimentinėse hibridinėse skaitmeninėse procedūrose.

Skysčio judesys plokštumoje gaunamas tik kaip skaičiavimų rezultatas: taigi pirmajame analizės etape nustatomas eksperimentinio vaizdo ir skaičiavimų, gautų tiriant skersinius skysčio paviršiaus judesius, atitikimas, o antrajame etape skaitmeniu būdu gaunamas skysčio judesys plokštumoje.

Pateikta spaudai 2005 02 28